Diagnostic and prognostic equations for the depth of the stably stratified Ekman boundary layer

By SERGEJ ZILITINKEVICH[1]*, ALEXANDER BAKLANOV[2], JUTTA ROST[1,3], ANN-SOFI SMEDMAN[1], VASILIY LYKOSOV[1,4] and PIERLIUGI CALANCA[5]

[1]*Uppsala University, Sweden*
[2]*Danish Meteorological Institute, Denmark*
[3]*University of Freiburg, Germany*
[4]*Russian Academy of Sciences, Russia*
[5]*Swiss Federal Research Station for Agroecology and Agriculture, Switzerland*

SUMMARY

Refined diagnostic and prognostic equations for the depth of the stably stratified barotropic Ekman boundary later (SBL) are derived employing a recently developed non-local formulation for the eddy viscosity. In well-studied cases of the thoroughly neutral SBL, the nocturnal atmospheric SBL and the oceanic SBL dominantly affected by the static stability in the thermocline, the proposed diagnostic equation reduces to the Rossby–Montgomery, Zilitinkevich and Pollard–Rhines–Thompson equations, respectively. In its general form it is applicable to a range of regimes including long-lived atmospheric SBLs affected by the near-surface buoyancy flux and the static stability in the free atmosphere. Both diagnostic and prognostic SBL depth equations are validated against recent data from atmospheric measurements.

KEYWORDS: Boundary-layer depth   Stable stratification

1. INTRODUCTION

The depth of geophysical (atmospheric and oceanic) turbulent boundary layers, h, is needed in a number of practically important problems such as pollution dispersion, wind engineering, air–sea interaction, weather prediction and climate modelling. The nature of these layers is critically dependent on the type of static stability: stable or unstable. In the present paper we consider the stably stratified Ekman boundary layers (henceforth referred to as SBLs), i.e. the boundary layers affected by the stable static stability and the earth's rotation. Moreover we focus on regular SBLs adjacent to the surface, in which the velocity shear is strong enough to maintain continuous turbulence holding out against negative buoyancy forces. The SBL depth is then specified as the turbulent-layer depth. The 'very stable boundary layers' (Mahrt 1998), characterized by intermittent turbulence concentrated in thin disconnected sub-layers—'pancake structures' and often affected by elevated shears, are not considered.

Although theoretical analysis is given in terms of the atmospheric SBL and experimental data are taken from atmospheric measurements, the proposed SBL depth formulation seems to be basically applicable to the stably stratified upper mixed layers in the ocean or lakes. In the latter layers, two specifically ocean/lake mixing mechanisms should generally be taken into consideration, namely, the Langmuir circulation and the surface wave breaking (see Kantha and Clayson 2000).

An inherent feature of the SBLs is that they cannot grow infinitely. Indeed, in stable stratification the production of the turbulent kinetic energy (TKE) is due to the velocity shear, and it is limited to $\int_0^h (\tau \cdot \partial \mathbf{u}/\partial z) \, dz \sim \overline{U} u_*^2$. Here, z is the height above the surface, h is the SBL depth, $\mathbf{u} = (u, v)$ is the wind velocity, $\tau = (\tau_x, \tau_y)$ is the vertical flux of momentum, $\overline{U}$ is the SBL mean wind velocity, and u_* is the friction velocity ($u_*^2 \equiv |\tau|_{z=0}$). At the same time the buoyancy flux, F_b, in the SBL is a decreasing

function of height. Given $F_b = F_{bs}(1 - z/h)^m$, where F_{bs} is the near-surface buoyancy flux, $m > 0$, the energy loss through overcoming the negative buoyancy forces becomes $\int_0^h F_b \, \mathrm{d}z \sim F_{bs}h/(1 + m)$, i.e. it increases with increasing depth of the layer. Here, $F_b = \beta F_\theta + 0.61g F_q$, F_θ and F_q are the fluxes of potential temperature, θ, and specific humidity, q, respectively; g is the acceleration due to gravity, $\beta = g/T_0$ is the buoyancy parameter, T_0 is a reference value of the absolute temperature, and the subscript 's' is used to mark the near-surface values. Comparing the energy production and the energy loss immediately puts an upper limit on the equilibrium depth of the SBL:

$$h < (1 + m)(\overline{U}/u_*)L \sim 10^2 \, L. \tag{1}$$

Here, $u_*/\overline{U}$ is the drag coefficient (a variable parameter with typical value ~ 0.02 in stable stratification), and

$$L \equiv -u_*^3/F_{bs} \tag{2}$$

is the Monin–Obukhov (MO) length-scale.

Alternatively, a restriction on the SBL depth is deduced by consideration of the bulk Richardson number,

$$\mathrm{Ri}_{\mathrm{SBL}} = h \Delta b/\overline{U}^2, \tag{3}$$

where Δb is the increment in buoyancy, $b = \beta\theta + 0.61q$, across the layer. The equilibrium SBL depth is estimated diagnostically from measured or modelled vertical profiles of the wind velocity and buoyancy, $u(z)$ and $b(z)$, assuming that the SBL evolves until $\mathrm{Ri}_{\mathrm{SBL}}$ reaches a standard critical value (e.g. Troen and Mahrt 1986). Taking the conventional value of $\mathrm{Ri}_{\mathrm{SBL}} \sim 1$ and the above typical value of $u_*/\overline{U} \sim 0.02$, Eq. (3) imposes an upper limit on the SBL depth:

$$h < (\mathrm{Ri}_{\mathrm{SBL}})^{1/2} \frac{\overline{U}}{u_*} \frac{u_*}{N} \sim 50 \frac{u_*}{N}, \tag{4}$$

where $N \equiv (\Delta b/h)^{1/2}$ is the SBL mean Brunt–Väisälä frequency.

The above analysis suggests that SBLs have a tendency to evolve towards a quasi-steady state characterized by equilibrium SBL depths. The inequalities Eq. (1) and Eq. (4) are derived, regardless, as concrete features of the SBL dynamics. The dimensionless coefficients on their right-hand sides (r.h.s.) are by no means constant. They depend on the full set of the SBL governing parameters including u_*, F_{bs}, the Coriolis parameter, f, and the Brunt–Väisälä frequency in the free flow above the SBL[*]. Derbyshire (1990) has given a detailed discussion of the concept of equilibrium or quasi-equilibrium geophysical (rotating) SBLs. As follows from the Galperin *et al.* (1989) advanced turbulence closure model for oceanic SBLs, the above limits are hardly applicable to non-rotating SBLs.

A number of depth-scales were proposed to measure the equilibrium SBL depth, h_E (see, e.g. an overview of the oceanic upper mixed layer models in Zilitinkevich *et al.* (1979)). The basic scales are:

(i) $h_E \propto u_*/|f|$, for the neutrally stratified SBL in a rotating fluid (Rossby and Montgomery 1935);

(ii) $h_E \propto L$, for the SBL dominantly affected by the surface buoyancy flux (Kitaigorodskii 1960);

---

[*] Considering baroclinic SBLs the list of the governing parameters should be extended to include the geostrophic-wind shears. The present paper focuses on barotropic SBLs.

(iii) $h_E \propto u_*^2/|f F_{bs}|^{1/2}$, for the SBL affected by the surface buoyancy flux and rotation (Zilitinkevich 1972);

(iv) $h_E \propto u_*/|f N|^{1/2}$, for the SBL affected by the free-flow stability and rotation (Pollard $et\ al.$ 1973);

(v) $h_E \propto u_*/N$, for the SBL dominantly affected by the free-flow static stability (Kitaigorodskii and Joffre 1988).

Having regard to the existence of the equilibrium SBL depths, it is conceivable that reasonably slow, gradual variations in the SBL depth should satisfy a relaxation equation

$$\frac{\mathrm{d}h}{\mathrm{d}t} = w_h - (h - h_E)/t_E, \tag{5}$$

where t_E is the relaxation time-scale (e.g. Mahrt 1981), w_h is the large-scale vertical velocity at the SBL upper boundary, $\mathrm{d}h/\mathrm{d}t = \partial h/\partial t + u\partial h/\partial x + v\partial h/\partial y$, u and v are the wind velocity components along the x and y axes, respectively.

For the neutrally stratified Ekman layer, dimensional analysis immediately suggests the expressions $h_E \propto u_*/|f|$ and $t_E \propto |f|^{-1}$ (Khakimov 1976). For the Ekman layer affected by the earth's rotation and the surface buoyancy flux, Mahrt (1981) gave a comprehensive review of early SBL depth models. It is likely that no prediction equation was proposed until now for the Ekman layer affected by the free-flow stability.

Equation (5) is not applicable to non-steady regimes with very fast deepening of the mixed layer against stably stratified undisturbed flow. Here, the growth of the SBL is often accompanied by discontinuities in the velocity and density profiles, and turbulent entrainment at the SBL outer boundary. Then the SBL depth equation becomes $\mathrm{d}h/\mathrm{d}t = w_h + w_e$, where w_e is the entrainment rate (e.g. Kato and Phillips 1969; Kraus 1977; Zilitinkevich $et\ al.$ 1979). Fast deepening of the oceanic SBL is observed when the wind stress at the water surface suddenly increases, with the result that the upper mixed layer as a whole strongly accelerates relative to the underlying thermocline. However, this sort of development is not typical of atmospheric SBLs. In the present paper it is not considered; this paper focuses on analysis of the equilibrium Ekman-layer depth and the relaxation time-scales. A comprehensive overview of modern knowledge about atmospheric SBLs is given by Smedman (1991), Mahrt (1998, 1999), Mahrt $et\ al.$ (1998).

2. EKMAN-LAYER SCALING

Considering the boundary-layer depth, h, the key point is the TKE production. In stable stratification it is controlled by the velocity shear. Given the eddy viscosity, K_M, the SBL depth-scale can be derived from the momentum balance equations. In the steady state Ekman layer these equations read (e.g. Garratt 1992)

$$f(v - v_g) + \frac{\partial}{\partial z}K_M\frac{\partial u}{\partial z} = 0, \quad -f(u - u_g) + \frac{\partial}{\partial z}K_M\frac{\partial v}{\partial z} = 0. \tag{6}$$

Here, u_g and v_g are the geostrophic wind components, $u_g \equiv -(\rho f)^{-1}\partial p/\partial y$ and $v_g \equiv (\rho f)^{-1}\partial p/\partial x$ (ρ is the air density and p is the pressure); whereas the components of the vertical flux of momentum along the horizontal x- and y-axes are given by $\tau_x = K_M\partial u/\partial z$ and $\tau_y = K_M\partial v/\partial z$ (the x-axis is aligned with the surface stress to make $\tau_y = 0$ at $z = 0$).

Velocity components, u and v, satisfy the boundary conditions

$$u = v = 0 \text{ at } z = 0; \quad u \to u_g, v \to v_g \text{ at } z \to \infty. \tag{7}$$

In the barotropic flow (when u_g and v_g are constant with depth), differentiating Eqs. (6) over z and then multiplying by K_M yields:

$$f\tau_y + K_M\frac{\partial^2 \tau_x}{\partial z^2} = 0, \quad -f\tau_x + K_M\frac{\partial^2 \tau_y}{\partial z^2} = 0, \tag{8}$$

where the momentum flux components, τ_x and τ_y, satisfy the boundary conditions

$$\tau_x = u_*^2, \tau_y = 0 \text{ at } z = 0; \quad \tau_x \to 0, \tau_y \to 0 \text{ at } z \to \infty \tag{9}$$

(remember, the x-axis is aligned with the surface stress).

At given K_M, Eqs. (8) and (9) immediately yield the vertical profiles of τ_x and τ_y, and eventually, the depth of the equilibrium Ekman layer, h_E. Moreover, it is evident that h_E is controlled by the portion of the flow where K_M is the *largest*. As a result, analysis of Eqs. (8) and (9) aimed at the derivation of the Ekman-layer depth-scale can be done substituting for the eddy viscosity K_M its *maximum* value, K_M^*, typical of the Ekman-layer interior and independent of height ($K_M^* = $ constant). Then employing the squared friction velocity, u_*^2, to measure the momentum flux and the familiar Ekman depth-scale, $(2K_M^*/f)^{1/2}$, to measure the height, and switching to the dimensionless variables:

$$\widehat{\tau}_x = \tau_x/u_*^2, \quad \widehat{\tau}_y = \tau_y/u_*^2, \quad \widehat{z} = z/(2K_M^*/f)^{1/2}, \tag{10}$$

Eqs. (8) and (9) become

$$\widehat{\tau}_y + \frac{1}{2}\frac{\partial^2 \widehat{\tau}_x}{\partial \widehat{z}^2} = 0, \quad -\widehat{\tau}_x + \frac{1}{2}\frac{\partial^2 \widehat{\tau}_y}{\partial \widehat{z}^2} = 0, \tag{11}$$

$$\widehat{\tau}_x = 1, \widehat{\tau}_y = 0, \text{ at } \widehat{\tau}_z = 0; \quad \widehat{\tau}_x \to 0, \widehat{\tau}_y \to 0 \text{ at } \widehat{z} \to \infty. \tag{12}$$

The problem given by Eqs. (11) and (12) is completely self-similar, i.e. it does not include any parameters. This immediately suggests that the only depth-scale in the problem is

$$h_* = (2K_M^*/f)^{1/2}. \tag{13}$$

Then h_E is nothing but a standard portion of h_*.

Notice that the solution to Eqs. (11) and (12), namely, $\widehat{\tau}_e = e^{-\widehat{z}}\sin\widehat{z}, \widehat{\tau}_y = e^{-\widehat{z}}\cos\widehat{z}$ is neither needed nor used in the present paper. Moreover, the assumption $K_M = $ constant, although well grounded in the derivation of the Ekman-layer depth-scale, would become completely unrealistic if one attempted to apply it to the velocity profiles or the resistance law.

3. SBL DEPTH EQUATIONS

To determine the eddy viscosity scale, K_M^*, it is sufficient to consider the eddy viscosity profile, $K_M(z)$, in the lower portion of the Ekman layer, the surface layer, where K_M is an increasing function of z. Here, the momentum flux can be taken as constant with depth ($|\tau| = u_*^2$). Then K_M is immediately expressed through the velocity gradient:

$$K_M = \frac{u_*^2}{\partial u/\partial z}. \tag{14}$$

In the upper portion of the Ekman layer K_M can only decrease.

In neutral stratification, the velocity gradient and the eddy viscosity profiles in the surface layer are $\partial u/\partial z = u_*/kz$ and $K_M = ku_*z$, where $k \approx 0.4$ is the von Karman constant. Hence the Ekman-layer eddy viscosity scale is $K_M^* \propto u_* h_*$. Then Eq. (13) immediately yields the well-known Rossby and Montgomery (1935) formula:

$$h_E^2 = \left(C_R \frac{u_*}{f} \right)^2, \tag{15}$$

where C_R is a dimensionless constant. Field data practically never correspond to thoroughly neutral stratification, which is why they can hardly be used to determine C_R. A rough estimate of $C_R \sim 0.5$ was obtained from lab experiments and large-eddy simulations by Zilitinkevich and Mironov (1996).

In stable stratification, two different regimes should be distinguished. The concern of the traditional theory is the nocturnal boundary layer. Its lower portion, the surface layer, is adequately described by the classical MO similarity theory (e.g. chapter 4 in Monin and Yaglom 1971). Here, the velocity gradient is

$$\frac{\partial u}{\partial z} = \frac{u_*}{kz} \left(1 + C_u \frac{z}{L} \right), \tag{16}$$

where L is given by Eq. (2), and C_u is an empirical constant estimated as $C_u \approx 2.1$ (Högström 1995). Equations (14) and (16) suggest that K_M turns to its maximum value in the upper portion of the surface layer, $K_M \to ku_*L/C_u$. So the eddy-viscosity scale is $K_M^* \propto u_*L$ and Eq. (13) yields the Zilitinkevich (1972) formula:

$$h_E^2 = \frac{C_S^2 u_* L}{|f|}, \tag{17}$$

where C_S is an empirical constant roughly estimated as $C_S \approx 0.7$ (see Fig. 4.37 in Caughey 1982). Nieuwstadt (1984) has given an elegant alternative derivation of this formula employing the concept of a limiting Richardson number in the upper portion of the SBL.

Equation (17) is well-supported by data from measurements in midlatitudinal nocturnal stably stratified boundary layers. However, at high latitudes this equation with $C_S \approx 0.7$ strongly overestimates the stable boundary-layer depth (King and Turner 1997; Handorf *et al.* 1999). A reasonable explanation of this discrepancy lies in the essentially different physical natures of the midlatitude and the high-latitude SBLs.

The traditional concept of local turbulence transport in stable stratification, underlying both the MO theory and Eq. (17), is adequate when applied to nocturnal boundary layers separated from the stably stratified free atmosphere by the so-called residual layer. During the first hours of the night, the latter keeps neutral stratification as a 'memory' of the daytime mixing, which prevents interactions between the boundary layer and the free atmosphere through gravity waves.

Clearly, no residual layers are observed on top of long-lived SBLs typical of high latitudes (Forrer and Rotach 1997; King and Turner 1997). Here, the stable stratification is observed throughout the troposphere, which is why the vertical wave propagation is not blocked. As a result the SBL turbulence becomes essentially non-local, and the traditional theories fail. Zilitinkevich and Calanca (2000) and Zilitinkevich (2001) have extended the surface-layer similarity theory taking into account possible distant interactions in the thoroughly stable stratification. They provided physical reasoning

and experimental data in support of an advanced velocity gradient formulation:

$$\frac{\mathrm{d}u}{\mathrm{d}z} = \frac{u_*}{kz}\left\{1 + C_u\frac{z}{L}(1 + C_{uN}\text{Fi})\right\}, \tag{18}$$

where Fi is the inverse Froude number*,

$$\text{Fi} = \frac{LN}{u_*}. \tag{19}$$

C_u is a known empirical constant ($C_u = 2.1$, after Hösgström 1995), and C_{uN} is a new constant introduced in the above papers and determined very approximately ($0.1 < C_{uN} < 0.4$).

Equations (14) and (18) give $K_M \to ku_*L/C_u(1 + C_{uN}\text{Fi})$. Then the eddy viscosity scale is $K_M^* \propto u_*L/(1 + C_{uN}\text{Fi})$, and the Ekman layer depth, h_E, becomes:

$$h_\text{E}^2 = \frac{C_S^2 u_* L}{|f|(1 + C_{uN}\text{Fi})}. \tag{20}$$

When Fi $\to 0$ it reduces to Eq. (17).

Interpolating between the reciprocals of Eqs. (15) and (20) yields

$$h_\text{E} = \frac{C_R u_*}{|f|}\left\{1 + \frac{C_R^2 u_*(1 + C_{uN}\text{Fi})}{C_S^2|f|L}\right\}^{-1/2}. \tag{21}$$

Equation (21) covers the whole range of the static-stability regimes from neutral to strongly stable. It reduces to the Rossby–Montgomery Eq. (15) in the thoroughly neutral stratification and to the Zilitinkevich Eq. (17) in the stably stratified midlatitudinal SBLs capped by neutrally stratified residual layers (Fi $\ll 1$).

Moreover, when the SBL is dominantly affected by the free-flow stability (Fi $\gg 1$), Eq. (21) reduces to the Pollard *et al.* (1973) formula:

$$h_\text{E} = \frac{C_S}{(C_{uN})^{1/2}}\frac{u_*}{(|f|N)^{1/2}}. \tag{22}$$

Equation (22) is widely used in physical oceanography. It describes the regime when the static stability in the thermocline affects the upper mixed-layer depth much more than the buoyancy flux through the water surface. Oceanographic estimates of the proportionality coefficient, designated here by $C_S/(C_{uN})^{1/2}$, fall in the range between one and two (e.g. part 2 in Kraus 1977; Zilitinkevich *et al.* 1979). This gives additional support to the more general Eq. (21). Indeed, meteorological estimates of $C_S = 0.7$ and $C_{uN} = 0.1/0.4$ yield $1 < C_S/(C_{uN})^{1/2} < 2$, in agreement with the above oceanographic estimates.

Estimating the Ekman-layer relaxation time, t_E, as a time-scale of the Brownian-type diffusion of momentum across the layer, yields $t_\text{E} \propto h_\text{E}^2/K_M \propto |f|^{-1}$. Then Eq. (5) becomes:

$$\frac{\mathrm{d}h}{\mathrm{d}t} = w_h - C_\text{E}|f|(h - h_\text{E}), \tag{23}$$

where C_E is an empirical dimensionless constant.

Given empirical constants C_R, C_S and C_{uN}, Eq. (21) expresses h_E through the familiar MO scale L (Eq. (2)) and the dimensionless number Fi (Eq. (19)). Then, given C_E, Eq. (23) allows calculation of the actual non-steady Ekman-layer depth, h.

---

* This parameter (designated by S in Zilitinkevich and Calanca 2000) quantifies the effect of the free-flow stability on the surface-layer turbulence.
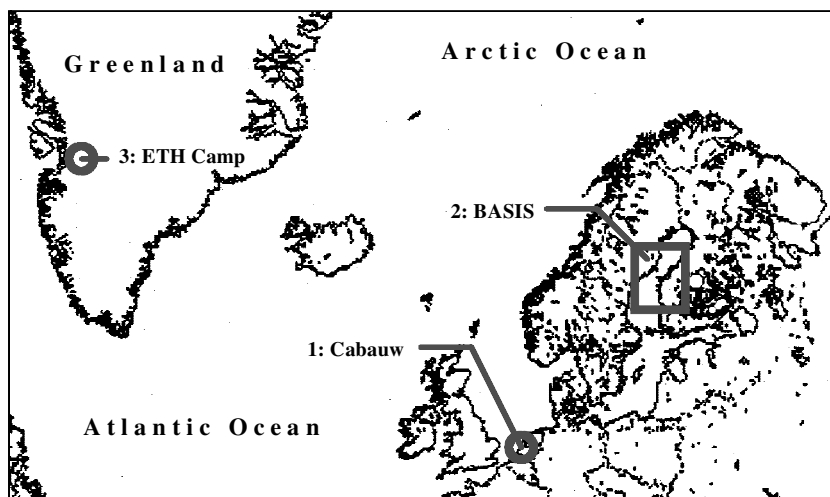
Figure 1. Sources of measurements used for empirical validation of the proposed SBL depth formulations: 1—the Cabauw research measurement station (Nieuwstadt 1984), 2—the area of the field experiment BASIS (Launiainen 1999), 3—the site of the ETH-Greenland expedition (Ohmura *et al.* 1992). See text for details.

4. EXPERIMENTAL DATA

Datasets used in this paper for empirical validation of the proposed SBL depth formulation are taken from three measurement sites (Fig. 1), namely:

- Cabauw measurement station (Nieuwstadt 1984; Van Ulden and Wieringa 1996);
- BASIS (Baltic Air–Sea–Ice Study) field experiment (Launiainen 1999); and
- ETH-Greenland expedition in summer 1991 (Ohmura *et al.* 1992).

(a) Cabauw

The Cabauw station of the Royal Netherlands Meteorological Institute (KNMI) is located in the western part of the Netherlands ($51°58'$N, $4°56'$E, 2 m above mean sea level (a.m.s.l.)) more than 50 km from the sea. The 200 m meteorological mast is surrounded by pastures and meadows, with typical surface roughness length for momentum $z_0 \approx 0.15$ m. The surface elevation changes do not exceed a few metres over 20 kilometres. In the present paper, data from measurements during the period 1977–79 were used. They included the mean vertical profiles measured at eight levels between 2 and 200 m, turbulence measurements, and SODAR measurements. For a detailed description of this measurement site and techniques see Vogelezang and Holtslag (1996).

As in the above paper, of the total set of 838 30-minute-average turbulence data samples, the cases were selected with negative turbulent fluxes of potential temperature (stable stratification) and SBL heights less than 180 m (to cover the entire SBL with the mast measurements and to calculate the Brunt–Väisälä frequency in the free atmosphere above the SBL). As distinguished from Nieuwstadt (1984), the cases with gravity waves were not filtered.

L and u_* were taken from the turbulence measurements in the surface layer. The measured SBL depth, h_{SBL}, was deduced from sodar measurements through analysis of the backscatter intensity profiles (Nieuwstadt 1984).
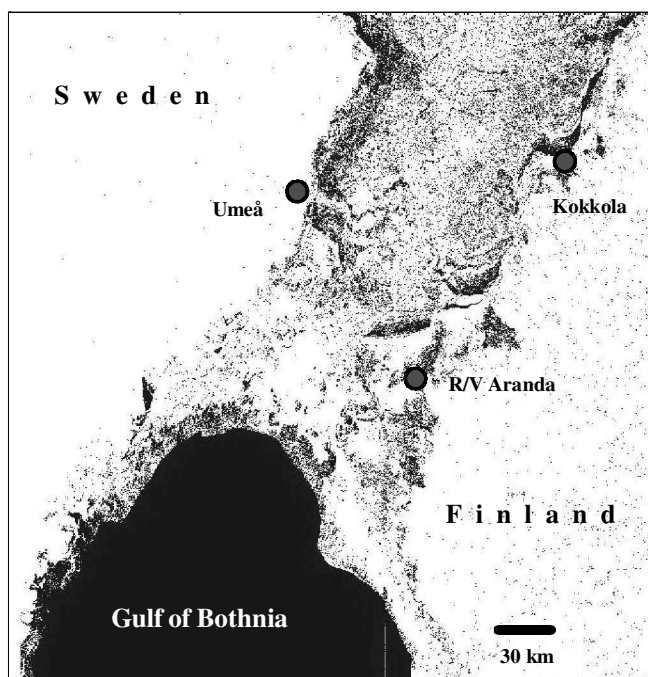
Figure 2.   Measurement sites, Umeå, Kokkola and R/V *Aranda*, in the field experiment BASIS, 16 February to 7 March 1998. The Radarset map (after Launiainen 1999) shows the border of the ice cover in the Gulf of Bothnia during the experiment.

The free-atmosphere Brunt–Väisälä frequency, N, was calculated from the temperature gradient in the layer adjacent to the SBL, taken from the mast-based mean profile measurements. Of the selected 196 cases of comparatively shallow SBLs, 65 cases corresponded to well-mixed SBLs on the background of pronounced free-flow stability, $N > 0.004$.

High-quality measurements at the Cabauw mast allowed quite accurate estimation of the SBL height. Their chief disadvantage is the lack of the mean profiles above 200 m. The nearest radiosonde station, De Bilt, is located 25 km north-east of the Cabauw mast, which is probably too far away for the purposes of this paper.

(b)   BASIS

The BASIS field experiment (Launiainen 1999) was performed from 16 February to 7 March 1998 at three sites in the Gulf of Bothnia region, namely, Umeå, Kokkola and R/V *Aranda* (Fig. 2). The landscapes around Umeå and Kokkola represent almost flat snow-covered meadows and low forests (Fig. 3). Here, the surface elevations change smoothly and do not exceed a few metres. At large scale, within 80 and 30 km from the sea on the Finnish and Swedish sides, respectively, they do not exceed 100 m. At R/V *Aranda* turbulent fluxes of heat, moisture and momentum were measured continuously over the frozen sea. Radio soundings were performed every sixth hour at all three sites.

The Umeå station was equipped with 30 m tower (Fig. 3) erected at the shoreline at Lövöudden (63°40.5′N, 20°24.0′E), which is a small peninsula about 25 km south of the town of Umeå on the Swedish east coast. There were undisturbed wind fetches over ice in the sectors 50–130° and 195–250°. Wind and temperature profiles were recorded at three heights. Turbulent fluctuations were measured with a Solent sonic anemometer

Figure 3.   Meteorological 30 m mast on ice at the Umeå station on the Swedish coast of the Gulf of Bothnia.

at 10 m height, and turbulent fluxes were calculated using the eddy-correlation method. The sonic anemometer was re-calibrated in a big wind-tunnel, and thus corrected for flow distortion prior to being installed on the tower. The calibration procedure is similar to that described by Grelle and Lindroth (1994). The sampling rate was 20 Hz.

The Kokkola station was situated on the sea ice in a bay near Kokkola at the Finnish coast ($63°95'$N, $23°09'$E). On a 10×10 m area four short masts were placed to measure standard parameters and turbulence. Wind speed was measured at 2 m, temperature and radiation at 1 m. Turbulence was measured at 3.5 m using a METEC sonic anemometer. There were at least 3 km open fetches in the sector 135–315°.

R/V *Aranda* was anchored in the landfast ice off the Finnish coast ($63°08.12'$N, $21°14.66'$E). A 10 m mast was erected about 300 m north-west of the ship to measure the temperature and wind profiles (five levels). Turbulence was measured at 2 m using a METEC sonic anemometer. This station had a sufficiently long open-ice fetch for all wind directions.

Figure 2 shows the Radarsat map of the Gulf of Bothnia. Here, the open water is black, the land is white, and the ice cover is textured (Launiainen 1999). Referring to this figure, the open water was more than 70 km distant from the measurement sites. The cases with winds blowing from open waters were excluded, to exclude convective internal boundary layers.

Data selection was based on the following criteria: (a) stable stratification near the ground ($L > 0$); (b) wind coming from undisturbed wind directions; (c) h_{SBL} clearly detected from the soundings (no internal boundary layers); (d) no front passing through or similar synoptic events.

Altogether 62 cases, 20 from Kokkola, 25 from R/V *Aranda* and 17 from Umeå, were selected for further analyses. Of these 62 cases, 48 exhibited a clearly stable stratification immediately above the SBL. For the other cases, the potential-temperature gradient has been set to zero. Due to the ice cover, the SBLs over the Gulf of Bothnia
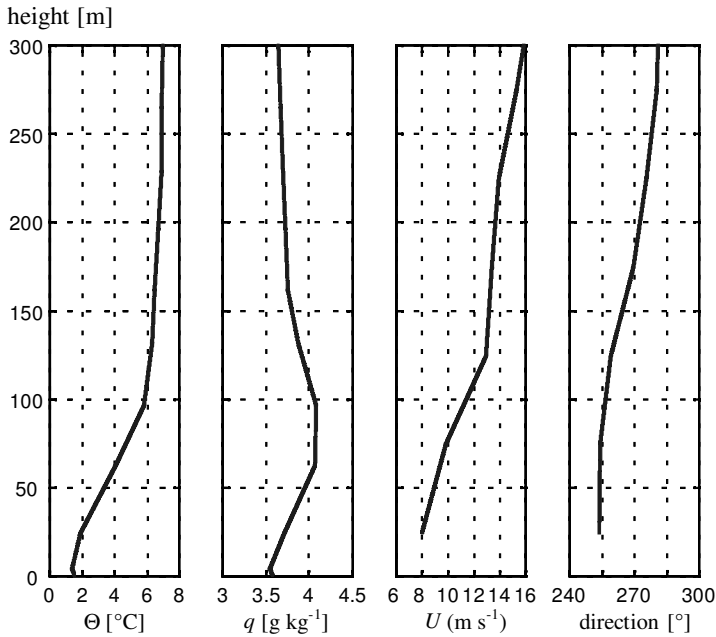
Figure 4.   Vertical profiles of potential temperature, specific humidity, wind speed and wind direction in a long-lived SBL: Umeå, 20 February 1998 at 1800 UTC. See text for details.

occurred during daytime. The soundings from the three stations were combined into one dataset. Earlier data divisions did not show large differences between the sites (considering winds coming from offshore).

L and u_* were taken from the surface turbulence measurements. The accuracy of turbulence measurements reduces due to inadequate statistical sampling. According to Dyer *et al.* (1982), for sampling periods of about one hour, the statistical error in determining the momentum flux is $\pm 15\%$.

N was deduced from the radiosonde temperature gradient in the layer adjacent to the SBL. In Fig. 4 this is the layer immediately above 100 m. For the surface-layer parameters, 30-minute mean values from the launching time of the radiosonde ± 15 minutes were chosen.

The SBL depth, h, was taken from the radiosonde profiles by the method of first temperature discontinuity (Hanna 1969; Wetzel 1982; Smedman 1991). In most cases the inversion depth was considered as the proxy for h_{SBL}. To avoid or to minimize errors in the determination of h in the thoroughly stable stratification, some cases with unclear temperature discontinuity/fracture were either rejected or reanalysed using the vertical profiles of specific humidity and wind velocity. The BASIS (as well as Cabauw) data were used to verify the diagnostic SBL depth formulation. Accordingly data from measurements in transition times were basically rejected.

(c)   *ETH-Greenland*

Data from the summer 1991 Swiss Federal Institute of Technology (ETH) Greenland expedition (Ohmura *et al.* 1992) were used for empirical validation of the prognostic SBL depth formulation. Here, measurements were carried out at the equilibrium line altitude at Paakitsoq ($69°34'25''$N, $49°17'44''$W, 1155 m a.m.s.l.) on the western Greenland ice sheet (Fig. 1). They included vertical profile measurements on the 30 m

meteorological mast, radiation measurements, upper air soundings, turbulence measurements, snow and ice investigations and synoptic observations.

Zilitinkevich and Calanca (2000) have already used (and briefly described) these data in their analysis of the surface-layer scaling for long-lived SBLs.

The mean wind speed and temperature were measured over 30-minute intervals at eight levels on the tower. Three sonic anemometers at 2, 10 and 30 m were used to record the high-frequency fluctuations of the wind speed and temperature. The sampling frequency was 21 s^{-1}.

The conditions in the lower troposphere were monitored twice a day with radiosondes. The temperature data were used to specify the height of the inversion layer (typically at some 70 to 200 m above the ground), assumed to be a first order estimate of the PBL height.

Consequently N was calculated from the potential-temperature profiles as a bulk frequency in the layer between h and 500 m above the ground. A time series of N with the same resolution (30 min) as time series for mean gradients and turbulent fluxes was produced from the twice-daily values by linear interpolation in time.

In 1991, stable or neutral stratification within the boundary layer occurred at the expedition site during the summer. The snow was melting so that the surface temperature could not rise above 0 °C, whereas the air was typically above freezing. This makes the expedition dataset especially convenient for empirical validation of the prognostic SBL depth formulation. The ETH-Greenland data for 24–25 July 1991 were chosen, because no residual layer was observed in this period.

5. EMPIRICAL VALIDATION OF THE PROPOSED SBL DEPTH EQUATIONS

For empirical validation of the proposed SBL depth equations (section 3) and estimation of dimensionless constants involved (especially the new constants C_{uN} and C_E) the following statistical criteria and parameters are used:

- the bias (the average difference between paired simulations and measurements);
- the root mean square error (r.m.s.e.);
- the correlation coefficient;
- the regression coefficient.

Figure 5 shows a preliminary comparison of the SBL depths: measured, h_{SBL}, and calculated, h_E, after Eq. (21) using the earlier estimates of the constants $C_R = 0.5$, $C_S = 0.7$ and $C_{uN} = 0.2$. Figure 5(a) is a scatter diagram for Cabauw and Fig. 5(b) for BASIS. Here a general correspondence is clearly seen, however, the spread of data points is quite pronounced. For the BASIS data the correlation coefficient is 0.56, the regression coefficient is 0.94, the bias is 4.2 m and the r.m.s.e. is 72 m. For the Cabauw data the correlation coefficient is 0.46, the bias is 9.5 m and the r.m.s.e. is 122 m.

As illustrated in Fig. 5(a), the scatter increases with increasing SBL height. Major errors occur at $h_{SBL} \sim 200$ m. This is only natural due to the lack of knowledge about the mean profiles in the vicinity of the SBL top, in particular, poor accuracy in the calculation of the free-flow Brunt–Väisälä frequency. Accordingly, the Cabauw data for $170 < h_{SBL} < 200$ are excluded from further analysis.

To validate Eq. (21), the Cabauw data on the SBL depth are presented in Fig. 6 as a plot:

$$\Phi = \left\{ \left(\frac{C_R u_*}{f h_E} \right)^2 - 1 \right\} \frac{|f| L}{u_*} \quad \text{versus} \quad \text{Fi} = \frac{NL}{u_*}. \tag{24}$$
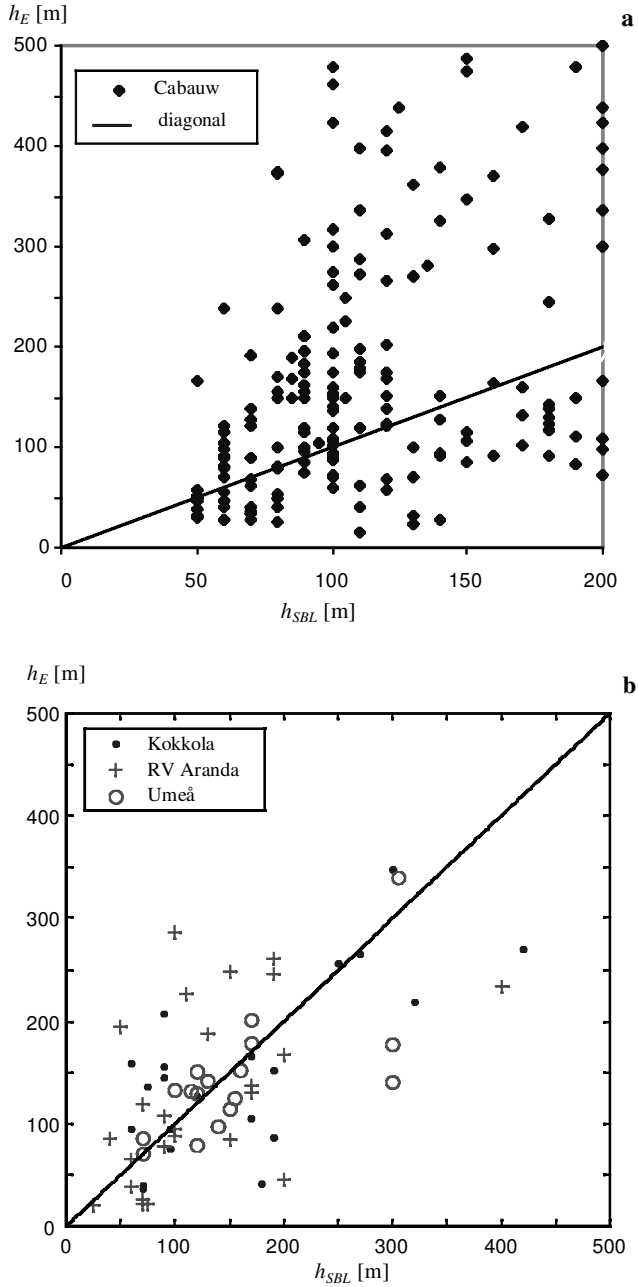
Figure 5. Comparison of the measured SBL depths, h_{SBL}, with h_E calculated using Eq. (21) with the earlier values of empirical constants $C_R = 0.5$, $C_S = 0.7$ and $C_{uN} = 0.2$: (a) for Cabauw, (b) for BASIS. See text for details.
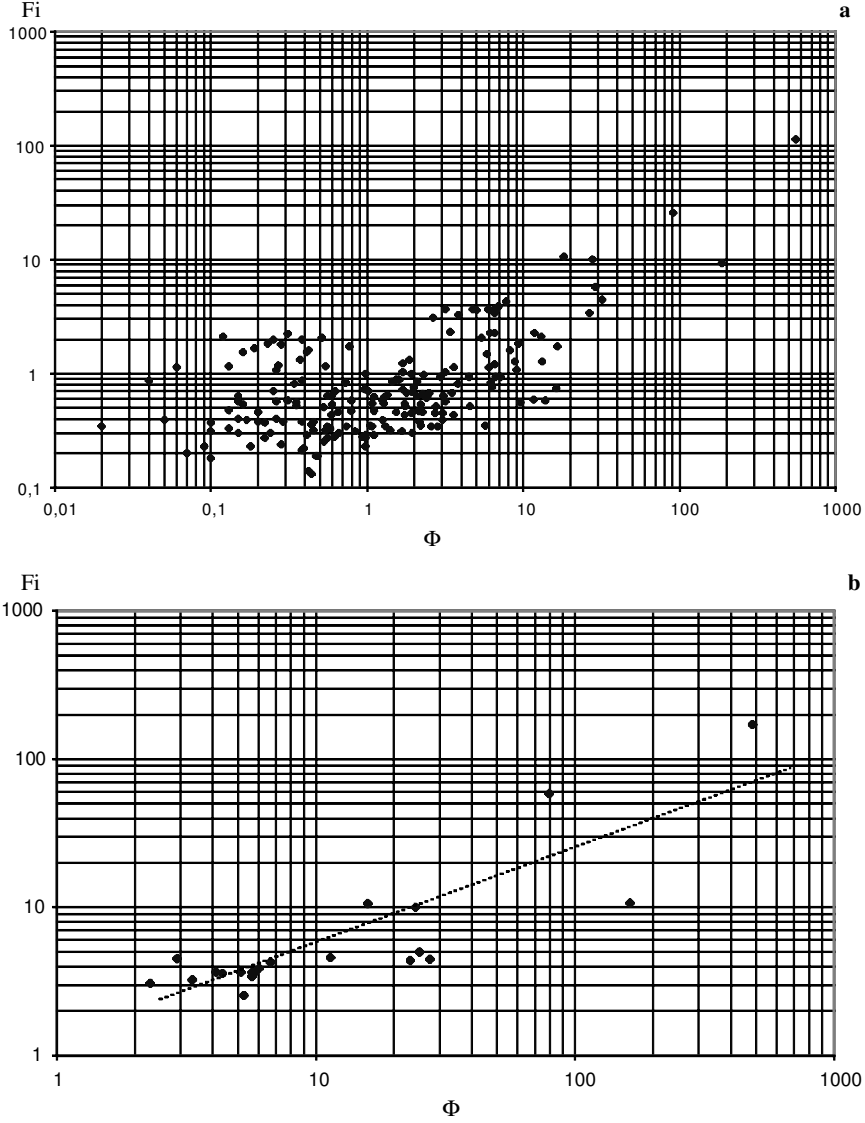
Figure 6. Logarithmic plot of the function Φ, Eq. (24), versus the inverse Froude number, Fi, for Cabauw: (a) all data with SBLs, (b) data with inversion-capped SBLs (Fi > 2.5). See text for details.

In Fig. 6(a) quite significant dependence of the function Φ on Fi is clearly seen. Here the correlation coefficient is 0.67. It can be further increased through more careful selection of data. Indeed, the similar dependence for the cases with strong free-flow stability (Fi > 2.5) presented in Fig. 6(b) clearly exhibits a higher correlation.

In further analysis the dimensionless constants C_S and C_{uN} are estimated using, separately, the data for near-neutral free flows (Fi $\to$ 0) and the data for near-neutral SBLs ($L \to \infty$). Resolving the neutral free-flow Eq. (17) for C_S, and substituting for h_E the observed h_{SBL}, yields:

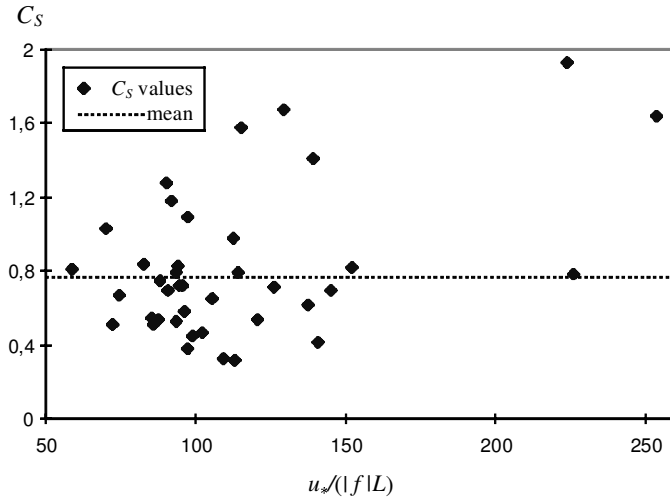$$C_S = \frac{h_{SBL}\sqrt{|f|u_*/L}}{u_*}. \tag{25}$$

Figure 7.   Dimensionless coefficient C_S, Eq. (25), versus the ratio $u_*/|f|L$ for the near-neutral free-flow regime (nocturnal SBLs), after the Cabauw data with Fi < 0.34. See text for details.

Empirical validation of Eq. (25) against the Cabauw, BASIS and ETH-Greenland data is shown in Figs. 7 and 8.

In Fig. 7 based on the Cabauw data, C_S is presented versus the stratification parameter $u_*/|f|L$. No systematic dependence is seen. C_S varies from 0.35 to 1.94 with the average value $\sim$0.75. The best correlation and minimum bias suggest the optimum value of $C_S = 0.79$.

Figure 8 shows the same analysis employing all three datasets. Here the selection criteria were Fi ≈ 0 and $u_* > 0.11$ m s^{-1} for BASIS, Fi < 0.3 for Cabauw and ETH-Greenland. In Figs. 8(b) and (c), an additional criterion $u_* > 0.08$ m s^{-1} was applied to the Cabauw data.

Figure 8(a) represents the three measurement sites of the BASIS experiment. The best-fit linear regression gives the first regression coefficient, the slope $\sim$0.7. However, the second regression coefficient, the intercept, is non-zero and gives a shift of the line $\sim$0.08. The forced linear regression with zero intercept gives $C_S = 0.55/0.61$ (Figs. 8(a) and (b)) depending on the selection criteria applied to the BASIS data.

Figure 8(b) presents similar estimations of the optimum value of C_S separately from each of the three datasets. As shown in Fig. 8(b), the Cabauw data give $C_S \approx 0.9$ and the ETH-Greenland data give $C_S = 0.6$. Figure 8(c) suggests the optimum value of $C_S \approx 0.62$ for all data taken together. Of these data, the ETH-Greenland data are probably less applicable to the equilibrium SBL depth problem due to significantly non-steady state and corresponding uncertainties of the interpolation of the SBL depth between the subsequent radio soundings. The most reliable estimate follows from Fig. 8(d), namely, $C_S = 0.69$ based on the BASIS and the Cabauw data.

In the earth's atmosphere, the near-neutral SBLs (with $L \to \infty$) are practically always capped by a stably stratified free flow, which is why the SBL depth is affected by the free-flow stability. Then the Rossby–Montgomery formula, Eq. (15), is not applicable. Instead, the SBL depth is expressed by a simplified version of Eq. (21)
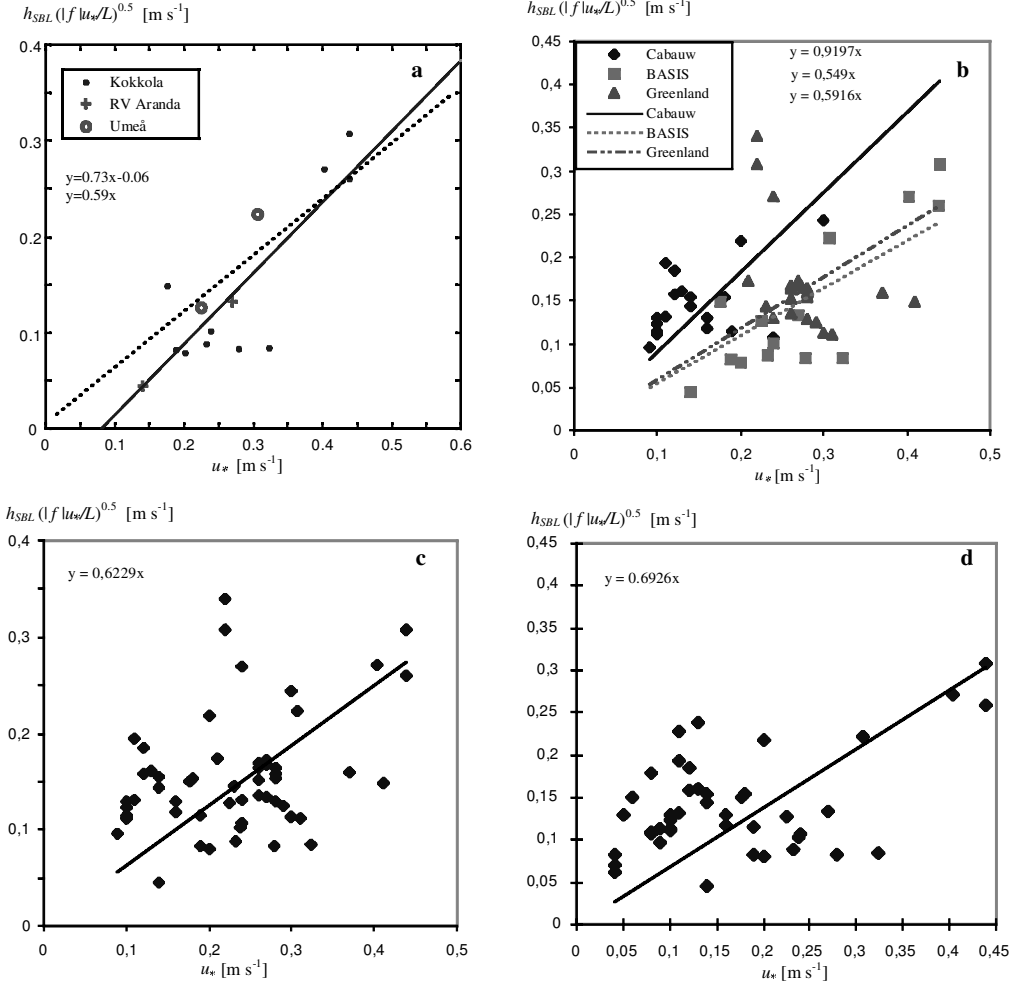
Figure 8. Re-estimation of the constant C_S from linear regression for the neutral free-flow regime (nocturnal SBLs), after the BASIS, Cabauw and ETH-Greenland data: (a) BASIS, (b) the three datasets, (c) joint regression for the three datasets, (d) joint regression for the Cabauw and BASIS data. See text for details.

neglecting the first (minor) term in braces:

$$h_E = \frac{u_*}{f} \left\{ \frac{C_S^2 |f| L}{u_* (1 + C_{uN} \text{Fi})} \right\}^{1/2}. \tag{26}$$

Here, a variable coefficient appears on the r.h.s. instead of the constant C_R in Eq. (15). Resolving Eq. (26) for C_{uN} and substituting the observed h_{SBL} for h_E yields:

$$C_{uN} = \frac{C_S^2 u_* L - h_{SBL}^2 |f|}{h_{SBL}^2 |f| \text{Fi}}. \tag{27}$$

Processing appropriately selected data from Cabauw (namely, those satisfying the conditions $L > 250$ m and Fi > 4), Eq. (27) yields $0.04 < C_{uN} < 0.9$. As shown in Fig. 9 a reasonably good correlation is observed in the range $0.25 < C_{uN} < 0.45$ with the best correlation at $C_{uN} \approx 0.35$.
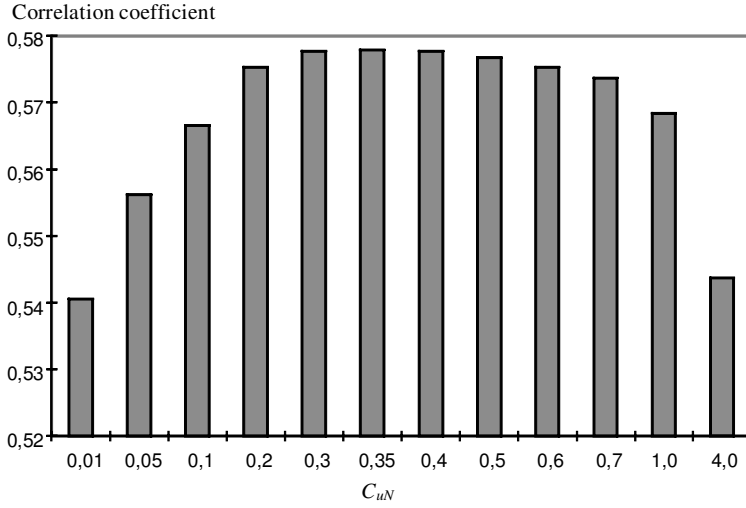
Correlation coefficient

Figure 9.   Correlation coefficients for different empirical estimates of the coefficient C_{uN} in Eq. (21), after the Cabauw data. See text for details.
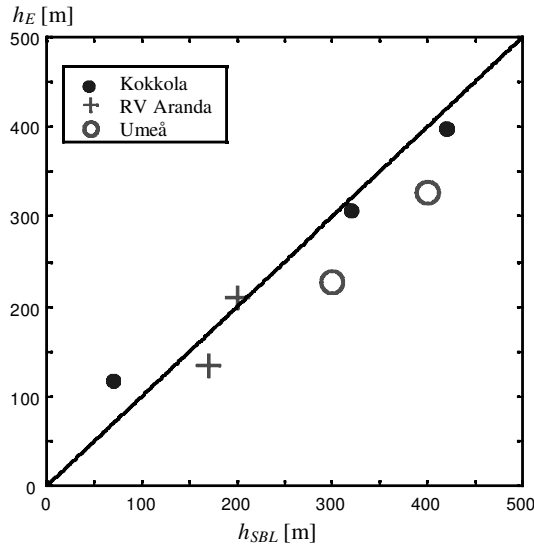

Figure 10.   Comparison of the measured SBL depths, h_{SBL}, with h_E calculated using Eq. (26) taking $C_S = 0.74$ and $C_{uN} = 0.1$, for BASIS. See text for details.

The similar regression analysis applied to data from BASIS selected to satisfy the condition Fi > 5, yields $0.04 < C_{uN} < 0.4$ with the recommended value of $C_{uN} \approx 0.1$. In Fig. 10, the SBL heights, h_E, calculated after Eq. (26) taking $C_S = 0.74$ and $C_{uN} = 0.1$ are compared with the BASIS empirical estimates of this height, h_{SBL}. This figure shows quite good agreement between h_E and h_{SBL}, with the correlation coefficient 0.92 and the regression coefficient 0.75. However, the number of data points is too small for reliable conclusions.

Recall that the Greenland data suggest the estimate $C_{uN} \approx 0.2$ (cf. Zilitinkevich and Calanca 2000), which lies just between $C_{uN} \approx 0.35$ (Cabauw) and $C_{uN} \approx 0.1$ (BASIS).
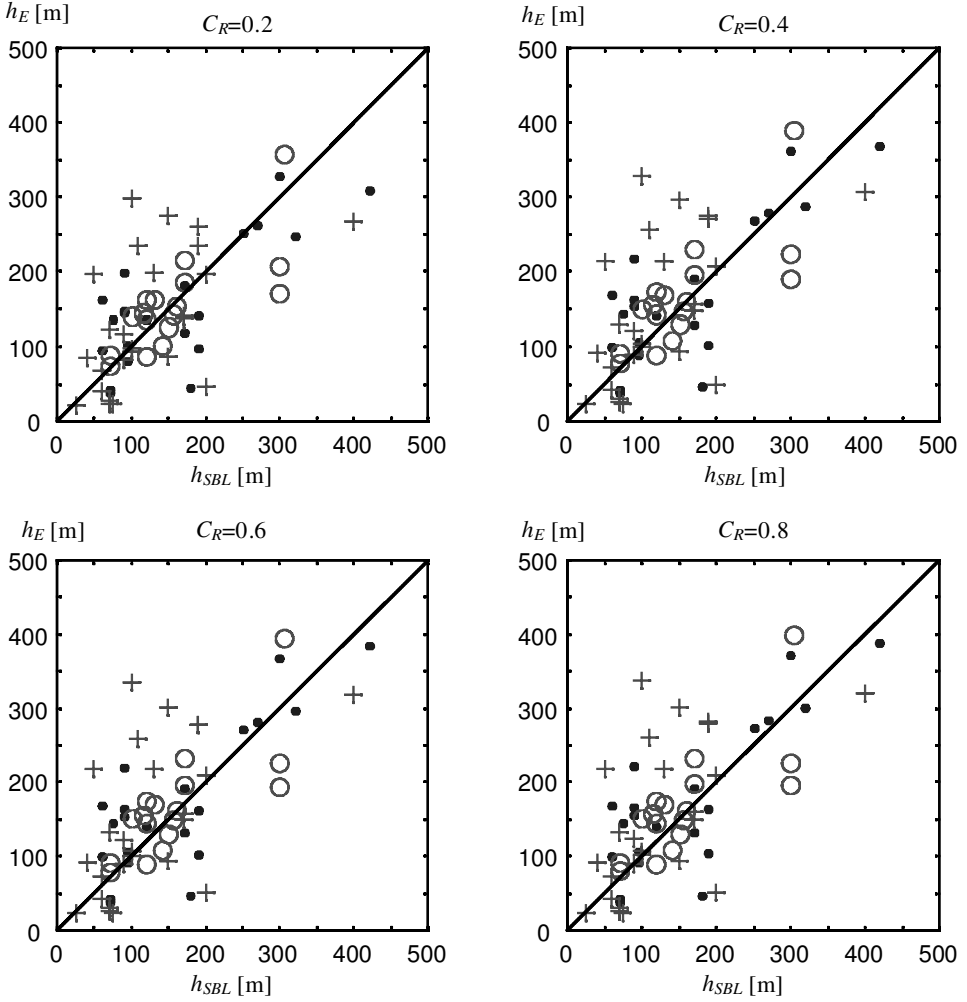
Figure 11. Comparison of the measured SBL depths, h_{SBL}, with h_E calculated after Eq. (21) taking $C_S = 0.74$, $C_{uN} = 0.1$ and $C_R = 0.2$, 0.4, 0.6 and 0.8, for BASIS. See text for details.

As already mentioned, the thoroughly neutral stratification in the lower atmosphere is practically never observed. Moreover, the general equilibrium SBL depth formulation, Eq. (21), is rather insensitive to the choice of C_R. Accordingly, Zilitinkevich and Mironov (1996) deduced an empirical value of $C_R = 0.5$ from large-eddy-simulation (LES) and lab-experiment data. In the present paper an attempt is made to re-evaluate this constant using atmospheric data.

Figure 11 compares theoretical values of h_E, calculated using Eq. (21) taking $C_R = 0.2$, 0.4, 0.6 and 0.8, with measured h_{SBL} taken from the BASIS data. Here, the graph with $C_R = 0.4$ exhibits a slightly better correlation than the three others. The similar analysis based on the Cabauw data yields $C_R = 0.35$. The same estimate, $C_R = 0.35$, was recommended recently by Zilitinkevich and Baklanov (2001).

The estimates of C_R from the BASIS data are presented in Table 1. Here, the bias and the r.m.s.e. reduce, and the regression coefficient increases, when C_R decreases from 0.8 and 0.2. At the same time the correlation coefficient decreases when C_R goes

TABLE 1. BIAS, r.m.s.e., REGRESSION AND CORRELATION COEFFICIENTS FOR VARIOUS C_R (TAKING $C_S = 0.74$ AND $C_{uN} = 0.1$)

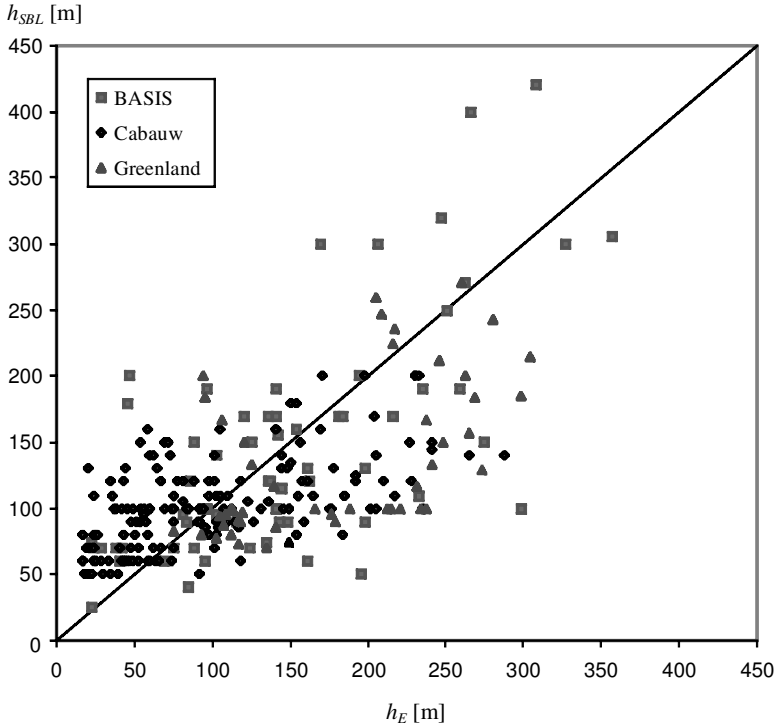| C_R	Regression coefficient	Correlation coefficient	Bias (m)	r.m.s.e. (m)
0.2	0.92	0.67	2.49	68.79
0.4	0.85	0.69	14.32	71.73
0.6	0.83	0.70	16.94	72.81
0.8	0.83	0.70	17.89	73.25

Figure 12. Comparison of the measured SBL depths, h_{SBL}, with h_E calculated after Eq. (21) taking refined values of the constants $C_R = 0.4$, $C_S = 0.74$ and $C_{u2} = 0.25$, for all data from BASIS, Cabauw and ETH-Greenland. See text for details.

below 0.4 and changes insignificantly when C_R falls within the range $0.4 < C_R < 1.0$. Considering all the above uncertainties and a low sensitivity of Eq. (21) to the choice of C_R, its tentatively recommended value is $C_R = 0.4$.

Figure 12 compares the measured and calculated SBL heights for different datasets: h_{SBL} is taken from measurements and h_E is calculated after Eq. (21) using refined constants, $C_R = 0.4$, $C_S = 0.74$ and $C_{uN} = 0.25$. The correlation coefficients are 0.669 for BASIS, 0.601 for Cabauw, and 0.547 for ETH-Greenland. Compared to Fig. 5 (based on the earlier estimates, $C_R = 0.5$, $C_S = 0.7$ and $C_{uN} = 0.2$) Fig. 12 clearly shows better performance. For the Cabauw data, the correlation coefficient becomes 0.60 (compared to 0.46), the bias becomes 6.21 m (compared to 9.53 m) and the r.m.s.e. becomes 50.89 m (compared to 122.35 m). For the BASIS data, the correlation coefficient becomes $r = 0.62$ (compared to 0.56) and the r.m.s.e. becomes 68.78 m (compared to 72.71 m). For the Greenland data, the r.m.s.e. becomes 75.01 m. Admittedly, on the
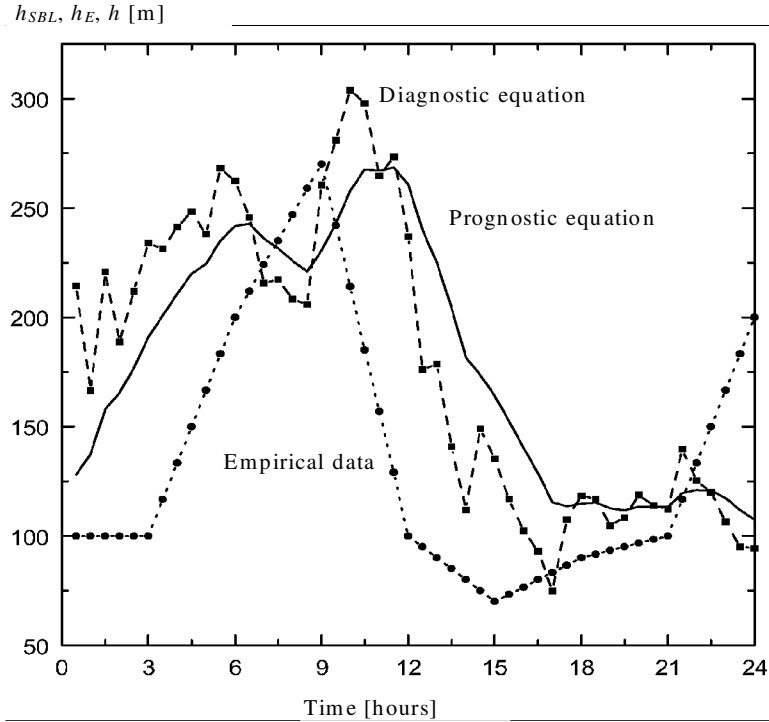
Figure 13. Temporal variation of the measured and calculated SBL depths: h_{SBL}—after the ETH-Greenland data (25 July 1991); h_E—after the diagnostic Eq. (21); and h—after the prognostic Eq. (23), taking $C_R = 0.5$, $C_S = 0.74$, $C_{uN} = 0.2$ and $C_E = 1$. See text for details.

background of the observed spread of data, the same comparison employing the earlier estimate of $C_{uN} = 0.2$ based on the surface-layer data (Zilitinkevich and Calanca 2000) is only slightly worse.

Considerable spread of data in Figs. 10–12 is quite understandable. Indeed, half-hour averages during non-steady situations might lead to underestimation or overestimation of the friction velocity or the sensible-heat flux, which inevitably results in strong uncertainty of the calculations. For the BASIS and the ETH-Greenland data, the SBL heights are deduced rather uncertainly from the radiosonde profiles. For the Cabauw data, when the SBL heights are close to the top of the mast, the calculation of the free-flow N becomes very uncertain.

The prognostic SBL depth equation, Eq. (23), was verified against data from the summer 1991 ETH-Greenland expedition (Ohmura *et al.* 1992). Here, the height of the inversion layer deduced from the mean temperature profile was identified with the observed h_{SBL}. Typically h_{SBL} lay between 70 and 270 m. Figure 13 compares the three estimates of the SBL height:

- h_{SBL} deduced from the above ETH-Greenland data;
- h_E calculated diagnostically after Eq. (21) with $C_R = 0.4$, $C_S = 0.74$ and $C_{uN} = 0.2$;
- h calculated after prognostic equation, Eq. (23), with $C_E = 1$.

The latter value of the relaxation-time constant C_E was obtained from best fitting of the prognostic-equation curve for experimental data. It is worth noticing that the

correspondence between the measured and calculated SBL height markedly worsened using $C_{uN} = 0.1$.

Summing up: empirical estimates of the dimensionless coefficients in Eqs. (21) and (23) are $C_R = 0.3/0.5$, $C_S = 0.6/0.79$, $C_{uN} = 0.1/0.35$ and $C_E = 1$. The values recommended for practical applications are $C_R = 0.4$, $C_S = 0.74$, $C_{uN} = 0.25$, and $C_E = 1$.

6.   CONCLUDING REMARKS

The proposed formulation for the depth of the barotropic stably stratified Ekman layer (SBL) consists of two operations, first, calculation of the equilibrium SBL depth from the diagnostic Eq. (21) and, second, integration of the relaxation-type prognostic Eq. (23) to obtain the actual SBL depth.

The diagnostic equation is derived employing the Ekman equations and a recently developed eddy viscosity model accounting for non-local features of long-lived SBLs. In this approach the free-flow Brunt–Väisälä frequency fits naturally into the scheme. This allows linking the meteorological and oceanographic SBL depth formulations.

Scaling analysis given in section 2 clearly shows that the dependence of the equilibrium Ekman-layer depth h_E on the Coriolis parameter f can never be neglected, no matter how strong the stratification. Thus from the momentum-balance standpoint any relationships linking h_E to the static-stability scales L or u_*/N cannot immediately be applied to the Ekman layer. It is most likely that the SBL in a non-rotating fluid can never achieve an equilibrium state.

Both diagnostic Eq. (21) and prognostic Eq. (23) are validated against atmospheric data. The major factors behind the spread of data points in all figures are the essential uncertainty of the observed values of the SBL depth and, probably, the mechanisms unaccounted for in the background Ekman-layer model (primarily the transition processes and baroclinicity).

Tentatively recommended values of the dimensionless coefficients in Eqs. (21) and (23) are $C_R = 0.4$, $C_{uN} = 0.25$, $C_S = 0.74$ and $C_E = 1$. To refine these coefficients (especially C_{uN}) further experimental studies are needed. Here, data from the turbulence and mean-profile measurements in the upper layer of the ocean would be very useful.

REFERENCES

Caughey, S. J.   1982   Observed characteristics of the atmospheric boundary layer. Pp. 107–158 in *Atmospheric turbulence and air pollution modelling*. Eds. F. T. M. Nieuwstadt and H. van Dop. D. Reidel, Dordrecht, the Netherlands

Derbyshire, S. H.	1990	Nieuwstadt's stable boundary layer revisited. *Q. J. R. Meteorol. Soc.*, **116,** 127–158
Dyer, A. J., Garratt, J. R., Francey, R. J., McIlroy, I. C., Bacon, N. E., Hyson, P., Bradley, E. F., Denmead, O. T., Tsvang, L. R., Volkov, Y. A., Koprov, B. M., Elagina, L. G., Sahashi, K., Monji, N., Hanasusa, T., Tsukamoto, O., Frenson, P., Hicks, B. B., Wesely, M., Miyake, M. and Shaw, W.	1982	An international turbulence comparison experiment (ITCE 1976). *Boundary-Layer Meteorol.*, **24,** 181–209
Forrer, J. and Rotach, M. W.	1997	On the turbulence structure in the stable boundary layer over the Greenland ice sheet. *Boundary-Layer Meteorol.*, **85,** 111–136
Galperin, B., Rosati, A., Kamtha, L. H. and Mellor, G. L.	1989	Modelling rotating stratified turbulent flows with application to oceanic mixed layers. *J. Phys. Oceanogr.*, **19,** 901–916
Garratt, J. R.	1992	*The atmospheric boundary layer*. Cambridge University Press, Cambridge, UK
Grelle, A. and Lindroth, A.	1994	Flow distortion by a Solent sonic anemometer: Wind tunnel calibration and its assessment for flux measurements over forest and field. *J. Atmos. Oceanic. Technol.*, **11,** 1529–1542
Handorf, D., Foken, T. and Kottmeier, C.	1999	The stable atmospheric boundary layer over an Antarctic ice sheet. *Boundary-Layer Meteorol.*, **91,** 165–189
Hanna, S. R.	1969	The thickness of the planetary boundary layer. *Atmos. Environ.*, **3,** 519–536
Högström, U.	1995	Review of some basic characteristics of the atmospheric surface layer. *Boundary-Layer Meteorol.*, **78,** 215–246
Kantha, L. H. and Clayson, C. A.	2000	*Small scale processes in geophysical fluid flows*. Academic Press, San Diego, USA
Kato, H. and Phillips, O. M.	1969	On the penetration of a turbulent layer into a stratified fluid, *J. Fluid Mech.*, **37,** 643–665
Khakimov, I. R.	1976	The wind profile in the neutrally stratified atmospheric boundary layer. Izvestiya, *Atmos. and Oceanic Phys.*, **12,** 628–630
King, J. and Turner, J.	1997	*Antarctic meteorology and climatology*. Cambridge University Press, Cambridge, UK
Kitaigorodskii, S. A.	1960	On the computation of the thickness of the wind-mixing layer in the ocean. Izvestiya, *Ser. Geophys.*, No, 3, 425–431
Kitaigorodskii, S. A. and Joffre, S. M.	1988	In search of simple scaling for the heights of the stratified atmospheric boundary layer. *Tellus*, **40A,** 419–443
Kraus, E. B.	1977	*Modelling and prediction of the upper layers of the ocean*. Pergamon Press, Oxford, UK
Launiainen, J. (Ed.)	1999	'BASIS-98 data report'. International BALTEX Secretariat, Publication No. 14. Available from Finnish Institute for Marine Research, PO Box 33, FIN-00931, Helsinki, Finland
Mahrt, L.	1981	Modelling the depth of the stable boundary layer. *Boundary-Layer Meteorol.*, **21,** 3–19
	1998	Stratified atmospheric boundary layers and breakdown of models. *J. Theor. and Comput. Fluid Dyn.*, **11,** 263–280
	1999	Stratified atmospheric boundary layers. *Boundary-Layer Meteorol.*, **90,** 375–396
Mahrt, L., Sun, J., Blumen, W., Delany, T. and Oncley, S.	1998	Nocturnal boundary-layer regimes. *Boundary-Layer Meteorol.*, **88,** 225–278
Monin, A. S. and Yaglom, A. M.	1971	*Statistical fluid mechanics: Mechanics of turbulence*. The M.I.T. Press, Cambridge, Massachusetts, USA
Nieuwstadt, F. T. M.	1984	The turbulent structure of the stable, nocturnal boundary layer. *J. Atmos. Sci.*, **41,** 2202–2216
Ohmura, A., Steffen, K., Blatter, H., Greuell, W., Rotach, M., Stober, M., Konzelmann, T., Forrer, J., Abe-Ouchi, A., Steiger, D. and Neiderbäumer, G.	1992	'ETH Greenland expedition: Progress Report No. 2, April 1991 to October 1992'. Department of Geography, Swiss Federal Institute of Technology, Zürich, Switzerland
Pollard, R. T., Rhines, P. B. and Thompson, R. O. R. Y.	1973	The deepening of the wind-mixed layer. *Geophys. Fluid Dyn.*, **3,** 381–404

Rossby, C. G. and   1935   The layer of frictional influence in wind and ocean currents. *Pap.*
    Montgomery, R. B.   *Phys. Oceanogr. Meteorol.*, **3**, No. 3, 1–101
Smedman, A.   1991   Some turbulence characteristics in stable atmospheric boundary
                                         layer flow. *J. Atmos. Sci.*, **48**, 856–868
Troen, I. and Mahrt, L.   1986   A simple model of the atmospheric boundary layer: sensitivity
                                         to surface evaporation. *Boundary-Layer Meteorol.*, **37**, 129–
                                         148
Van Ulden, A. P. and Wieringa, J. 1996   Atmospheric boundary layer research at Cabauw. *Boundary-
                                         Layer Meteorol.*, **78**, 39–69
Wentzel, P. J.   1982   Toward parameterization of the stable boundary layer. *J. Appl.
                                         Meteorol.*, **21**, 7–13
Vogelezang, D. H. P. and   1996   Evolution and model impacts of the alternative boundary layer
    Holtslag, A. A. M.   formulations. *Boundary-Layer Meteorol.*, **81**, 245–269
Zilitinkevich, S. S.   1972   On the determination of the height of the Ekman boundary layer.
                                         Boundary-Layer Meteorol., **3**, 141–145
                                 2001   Third-order transport due to internal waves and non-local turbu-
                                         lence in the stably stratified surface layer. *Q. J. R. Meteorol.
                                         Soc.* in press
Zilitinkevich, S. S. and   2001   'Calculation of the height of stable boundary layers in opera-
    Baklanov, A.   tional models'. DMI scientific report. Available from the
                                         Danish Meteorological Institute, Lyngbyvej 100, DK-2100
                                         København Ø, Denmark
Zilitinkevich, S. and Calanca, P. 2000   An extended similarity-theory for the stably stratified atmospheric
                                         surface layer. *Q. J. R. Meteorol. Soc.*, **126**, 1913–1923
Zilitinkevich, S. S. and   1996   A multi-limit formulation for the equilibrium depth of a sta-
    Mironov, D. V.   bly stratified boundary layer. *Boundary-Layer Meteorol.*, **81**,
                                         325–351
Zilitinkevich, S. S., Chalikov, D. V. 1979   Modeling the oceanic upper layer. *Oceanol. Acta*, **2**, 219–240
    and Resnyansky, Yu. D.